

Study and Data Acquisition Plan Induced Seismicity in Groningen

Addendum to version 5 July 2020

November 2020

Jan van Elk, Dirk Doornhof and Jeroen Uilenreef

Study and Data Acquisition Plan 2020 – Addendum
Close-out Report

Contents

Executive Summary.....	4
Wierden	4
Ground Motion Prediction.....	4
Seismological Model	4
Introduction	5
Wierden Project	6
Wierden in Groningen.....	6
Characterisation of the Wierden	7
Impact of the wierden on ground motions.....	9
Soil-structure Interaction.....	10
Local Site Response.....	11
Further work	13
Ground Motion Prediction.....	14
Seismic data validation	14
Shallow formation Properties	17
Shear wave velocity	17
Damping.....	19
Further Work.....	20
Seismological Model	22
Areal and temporal distribution of earthquakes	22
Further Work.....	22
Stress-Dependent Magnitudes	22
Further Work based on discussion with the Assurance Panel.....	23
References	25

Executive Summary

In this addendum to the Study and Data Acquisition Plan 2020, further development and further studies are described for three research areas as requested by SodM (Letter 15 September 2020, “Beoordeling Study and Data Acquisition Plan, update 1 juli 2020”):

- Assessment of hazard on dwelling mounts (wierden),
- Progress of the development of the 7th version of the ground motion prediction method,
- Further improvements of the seismological model.

Wierden

An extensive measurement campaign followed by studies has been executed to characterise the wierden in the Northern Netherlands and model the impact of the wierden on the amplification of seismic motions. These wierden were constructed using locally available soil materials and cattle manure.

Studies showed that soil-structure-interaction is only marginally impacted by the wierden. However the wierden does result in an additional amplification of seismic motion. A period-dependent additional amplification factor (multiplier) will be developed.

Ground Motion Prediction

Development of ground motion prediction methodology version 7 is in progress. In this report the results of the work packages that have been completed are reported. These are the rigorous screening of the seismic records obtained in Groningen, development of the database of seismic records and the characterisation of the shallow geological layers in Groningen, in particular the characterisation of soil damping.

Planning and progress on the remaining works packages in discussed.

Seismological Model

Recent developments in geophysical analysis of seismic data allows the source mechanism and rupture development of the earthquakes to be assessed. This new dataset offers an opportunity to improve the seismological model. The availability of the rupture direction for a large set of earthquakes might favour one set of geological faults over others, impacting the areal distribution of the earthquakes.

In addition, the assurance panel suggested some further analysis in support of the magnitude distribution of the earthquakes.

Introduction

On 11th February 2019, NAM submitted the fourth edition of the Study and Data Acquisition Plan (Ref. 1) to the Ministry of Economic Affairs and Climate (Min EZK) and the regulator (SodM). Together with an addendum this received the approval (“tengenoegen van de IGM”) of SodM on 17th December 2019 (Ref. 2 and 3). With this approval NAM was also requested by SodM to submit a further fifth edition.

On the 30st July 2020, this fifth edition of the Study and Data Acquisition Plan (Ref. 4 to 7) was submitted to the regulator and the Ministry. In September 2020 this report received the approval of SodM (Ref. 8) and was published on the NAM webpage “onderzoeksrapporten”. Furthermore, SodM requested an addendum to the Study and Data Acquisition Plan - 2020 to be submitted before 1st November 2020.

This addendum should address progress and plans for further study on three ongoing studies:

- The incorporation of the impact of dwelling mounts (wierden) on the hazard,
- The development of the Ground Motion Prediction Methodology (GMM V7) and
- Follow-up on suggestions from the assurance panel regarding the seismological model.

The current report describes the latest progress and further studies plans on these three area of research.

Wierden Project

Wierden in Groningen

In the Groningen area many of the older buildings are located on dwelling mounts (terpen in Dutch and locally called wierden). These are elevated areas build by humans, which served to protect buildings and people against floods. They are relatively small and have an elevation of a few metres above their surroundings. The wierden were built from the Middle Iron Age to the late Medieval Period. Many of the village centres (so called terpdorpen) and older and therefore potentially more vulnerable heritage buildings are located on these wierden (Fig. 1). In total some 2,862 buildings in the seismically active area (of the some 157,956 buildings in the exposure database or 1.8%) are located on these wierden. The wierden are therefore of interest for the hazard and risk assessment.

The wierden were constructed from locally available surface material (e.g. sods cut from surrounding salt marsh deposits and soil from digging ditches around the wierden) and manure from cattle. The composition of the wierden is therefore very heterogeneous and different from the surroundings.



Figure 1 Examples of two wierden (terpendorpen) left Westeremden en right Middelstum

In 2016, a study was carried out (Ref. 9 to 11) to inventorise the Wierden in the Groningen area and prepare a selection of the wierden for a measurement campaign to better characterise the wierden and model their response to earthquake movements. While the local surroundings provided an indication of the natural materials used in the construction of the wierden, the contribution from manure could not be established, but was thought to be substantial. In total nine representative wierden were selected for the measurement and characterisation campaign; Groot-Maarslag, Amsweer, Beswerd, Biessum, Ezinge (Zuidweg 1), Ezinge (Zuidweg 3), Fransum, Grote Houw and Helwerd. The aspects considered in selecting these wierden were:

Regional: Include all physiogeographical regions within the coastal zone, as locally available material was used in the construction of the wierden.

Study and Data Acquisition Plan 2020 – Addendum Close-out Report

Wierden Size: Ranging from small, single farm wierden to medium and large wierden. Manure content will vary with the size of the wierden (large wierden contain lower proportions of manure). Heritage buildings are more often found on the medium to larger wierden.

Sample size: Variability between wierden (even in close proximity) is large.

Preference for wierden with less buildings: Anthropogenic noise and the presence of building foundations and sewage systems might complicate data gathering.

Quarrying of the wierden: In the late 19th and early 20th century wierden were commercially quarried as fertiliser. Extensively quarried wierden were excluded from this study.

Characterisation of the Wierden

A measurement campaign was carried out to assess the lithological composition and typical shear wave velocities of wierden in the province of Groningen. It consisted of archaeo-lithological hand coring and micro-seismic measurements on a representative set of nine wierden. By combining these datasets, a statistical representation of lithoclasses and their distribution within the wierden body was created, providing the input for the development of the Ground Motion Prediction Methodology. Both active and passive surface wave techniques have been used. Hammer and accelerated weight drop sources were used for active Rayleigh-wave acquisition and a shear wave vibrator was used for active Love-wave acquisition.

The geophysical measurements were performed by Rossingh Geophysical. Multi-channel analysis of surface wave (MASW) data were collected and then developed into 1D models for Vs, using the passive source Rayleigh- and Love-wave data, accelerated weight drop (1D MASW) and 2D MASW data. The data were also developed into 2D Vs profiles using the active source Rayleigh- and Love-wave data collected along approximately 120 m long transects on each wierden. Geophysical processing was carried out by Geovision.

The wierden Groot Maarslag was the first pilot location to be investigated late 2017. A seismic receiver network consisting of four long lines arranged in a star-shaped pattern was placed at a small distance from the wierden as a reference (Fig. 2). On the wierden another star-shaped network was placed, with sensor on the main lines placed at short 1 m intervals. This main line extended beyond the boundary of the wierden. On the wierden and in the surrounding area, cores were acquired (see figure 4). The coring was carried out in cooperation with RAAP Archeologisch Adviesbureau. For each of the wierden, the proportions of lithoclasses shear wave velocity and variability and 2D profiles of Vs from Rayleigh-waves were prepared (Fig. 4).

Study and Data Acquisition Plan 2020 – Addendum
Close-out Report

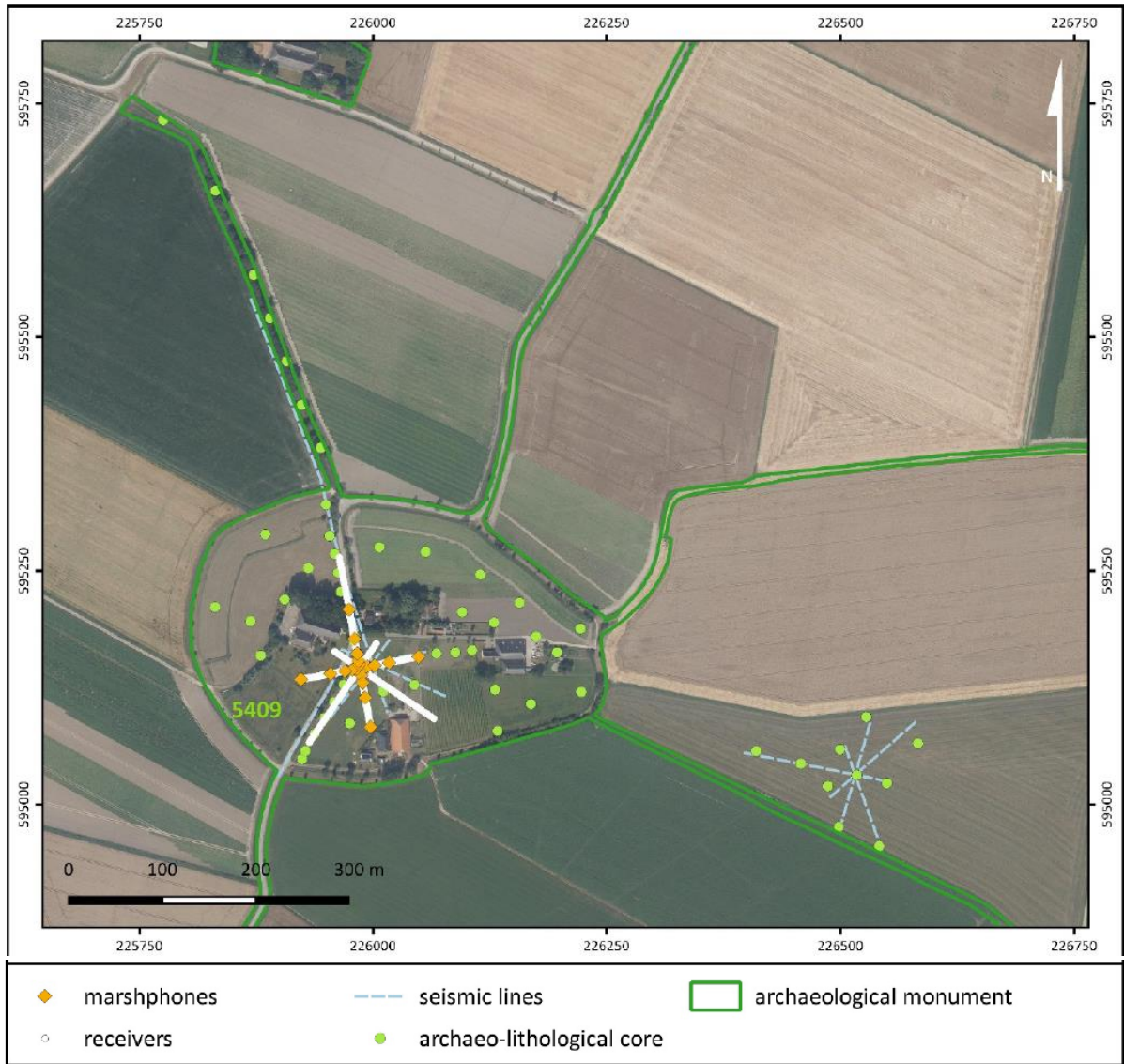


Figure 2 Location Groot Maarslag (pilot project). Overview of seismic lines, seismic receivers and archaeo-lithological cores.

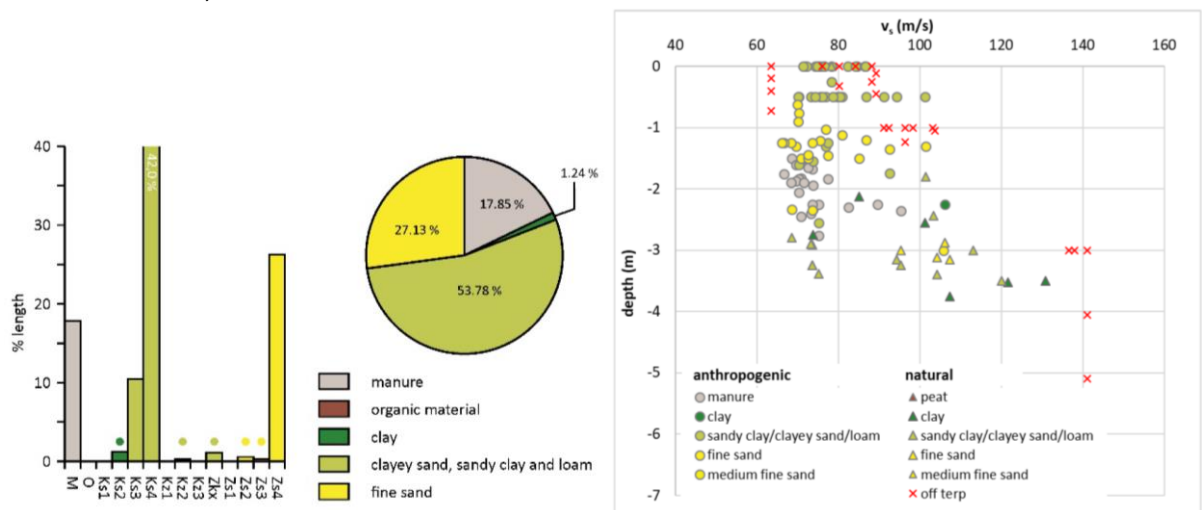


Figure 3 Results of characterisation of wierden Groot Maarslag. Left: Wierden lithoclass proportions of Groot Maarslag. Frequency distribution NEN5104 lithoclasses and manure. Dots denote values < 2% and percentages of GeoTOP lithoclasses. Right: Vs values per lithoclass plotted against depth below soil surface for Groot Maarslag.

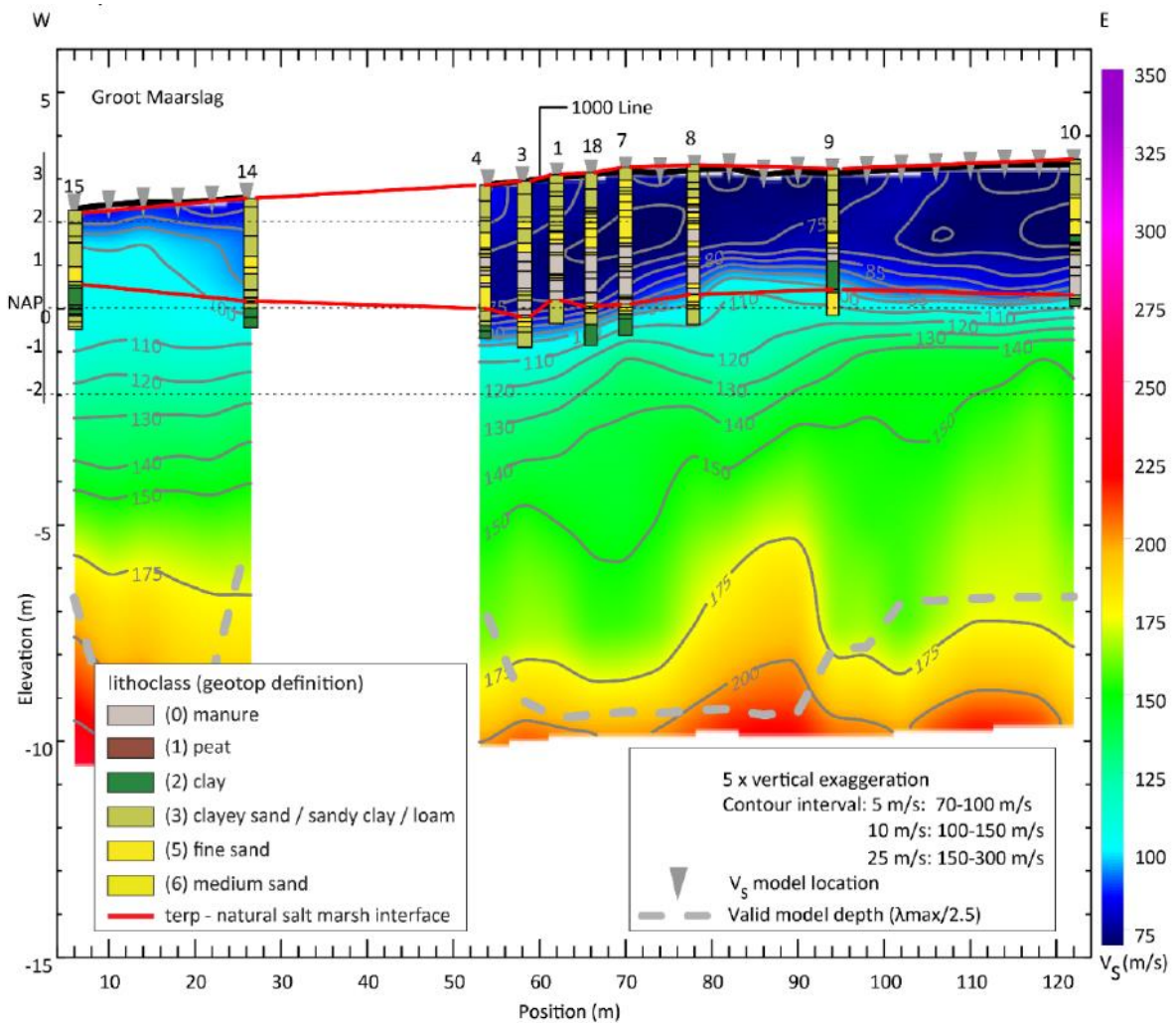


Figure 4 Rayleigh wave 2D profile with archaeo-lithological corings for Groot Maarslag (on wierden; adapted after Geovision, 2019b). The red lines indicate the anthropogenic wierden material.

After processing of the data acquired at the Groot Maarslag location, several changes were made to the receiver array. Analysis of the V_s measured at the nine wierden indicated that for each lithoclass the order of the V_s values per wierden seemed very similar. For instance V_s was for Amsweer and Biessum consistently on the low side and for Grote Houw and Helwerd on the high side. This points towards a “terp-effect” (or dependency on the specific wierden) in addition to the lithoclass effect. In addition, to depth and lithology the wierden itself is a predictor for V_s .

Using the model of the shear wave velocity based on depth and lithoclass, it is possible to extrapolate the work to other wierden in the area. By first assessing the lithology of individual wierden, either by coring or by the method presented (Ref. 12) and secondly using the regression equation as model, it is possible to calculate typical V_s values for each individual wierden. By measuring shear wave velocities and detailed lithoclass composition, we now have a good overview of the ‘typical’ wierden and the possible variations between different wierden. The wierden study provides a characterisation of typical wierden in the province of Groningen, which can be used as input for an updated GMM to further assess the possible impact of the anthropogenic wierden composition on earthquake amplification.

Impact of the wierden on ground motions

The wierden can impact the movement of a building located on the wierden through two mechanisms:

Study and Data Acquisition Plan 2020 – Addendum Close-out Report

- Change in the soil-structure interaction; the transfer of the ground movement into the foundations of the building.
- Amplification of the ground movement. Because the material the wierden is constructed from is relatively soft, it is expected that the dwelling mounts might cause an amplification of ground movement.

In the next two sections these two potential ways the presence of a wierden can impact the hazard will be discussed.

Soil-structure Interaction

Based on representative soil profiles for wierden the impact of the wierden on the transfer of the ground movement into the foundations of buildings was studied (Ref. 13 and 14). As the soil-structure interaction is incorporated in the fragility curves for the different building typologies, two sets of fragility curves were developed. The fragility curves were developed for these typologies when located on a wierden and compared to the fragility curve for the same typologies not located of a wierden. For this modelling exercise nine typologies were selected which together cover 88% of the building located on a wierden (2,532 of the 2,880 building located on a wierden).

Conclusions of this modelling study are:

- For the vulnerability classes with a higher number/percentage of buildings on wierden soil (i.e. detached/farm houses – URM6L, URM8L, URM7L, URM1F_HA, URM1F_HC) the changes in fragility are essentially negligible (the one case where a very slight fragility increase is observed concerns in any case a high strength class – URM7L).
- A slightly more noticeable, even if always very modest, change (decrease) in fragility is observed for terraced house vulnerability classes (URM3L, URM4L) – however only 0.35% of such buildings are founded on a wierden.

In summary, these results indicate there is no requirement to derive and then use site-specific fragility functions for the vulnerability classes to capture de impact of wierden on the soil-structure interaction with buildings located on wierden.

Study and Data Acquisition Plan 2020 – Addendum Close-out Report

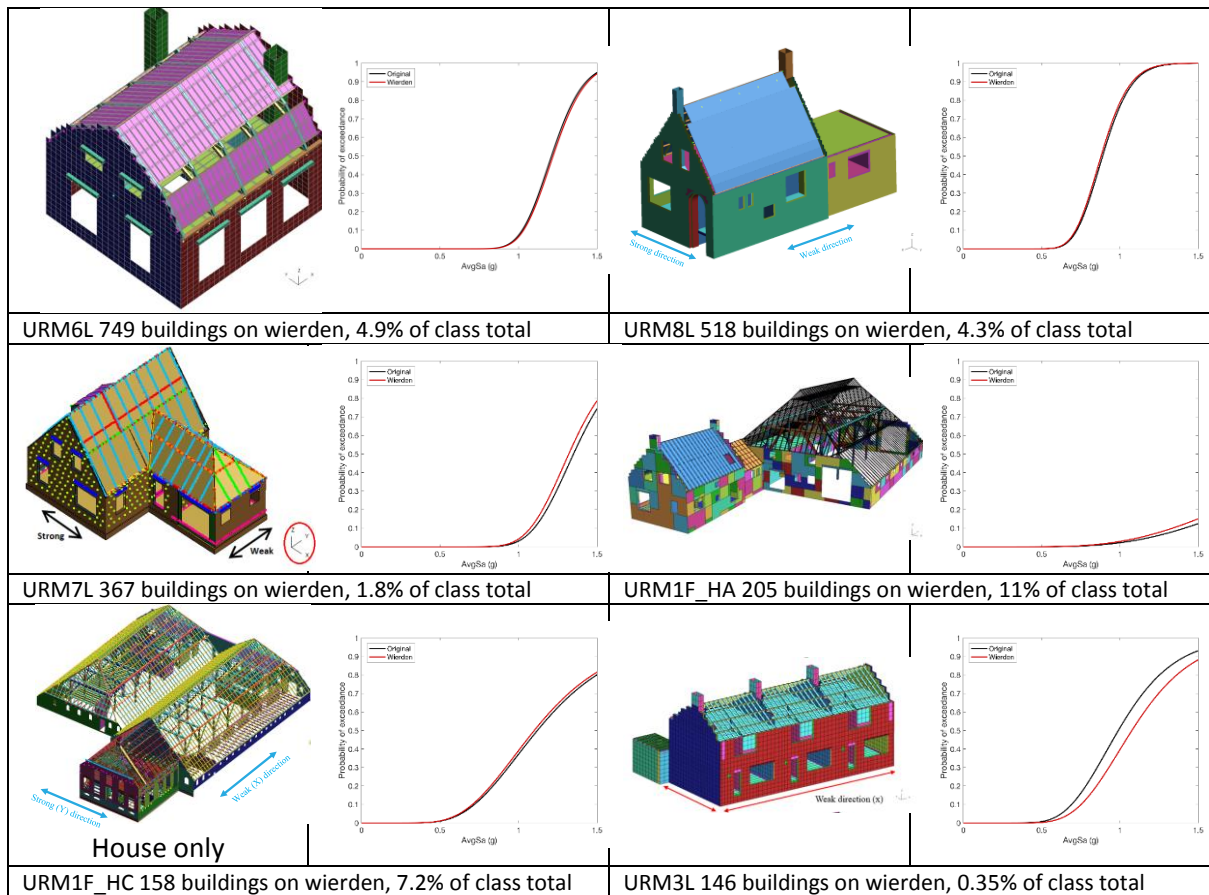


Figure 5 Comparison of fragility curves for a building typology located on and off a wierden.

Local Site Response

For the selected wierden, site response analyses were performed in order to define the typical wierden response. The same approach was used as in the development of the site response for the ground motion prediction methodology, which is described in Ref. 15 and 16. The site-response analyses were performed using 1-D models for vertically propagating shear-waves from a reference located at 16 m depth. This was done using Random Vibration Theory (RVT) in the frequency domain. The frequency-domain equivalent linear approach was used as implemented in the software program STRATA. The input for the STRATA calculations consist of soil profiles, input motions and soil properties dictating the shear degradation modulus reduction and damping curves as a function of strain. The methods used are based on those also used in the development of GMM V6 (Ref. 17 to 24).

The amplification factors for the three wierden located within the GMM area for a representative motion are shown in Fig 6. The general response is similar, but the absolute values are different. Amsweer generally has the highest Amplification Factor (AF), Helwerd the lowest and Biessum falls in between. The variation between the three wierden is larger than within the wierden. Figure 6 also shows the average AF for each wierden and the average of the three wierden, together with the average of the corresponding GMM soil profiles. Not only is there a difference in AF, but also a shift in the peak period. The difference suggests that the AF penalty function for buildings situated on wierden should be period- or frequency-dependent.

Study and Data Acquisition Plan 2020 – Addendum
Close-out Report

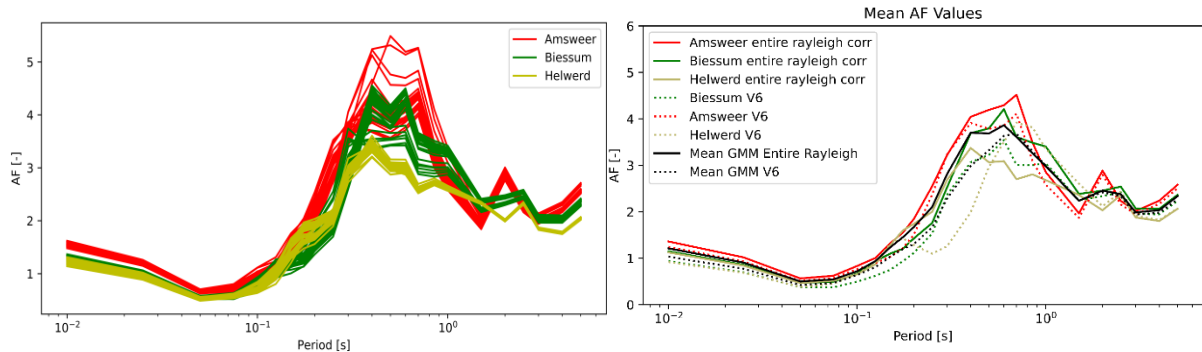


Figure 6 Left: Amplification Factors (AF) for all GMM wierden profiles for one of the selected motions. Right: Mean Amplification Factors for the local data (solid line) compared to the model data (dotted line) showing the average AF for the four motions dominating the seismic hazard.

For each of the local data coordinates, the AF from the GMM model V_s and soil column (Kruiver et al., 2017a and 2017b) was calculated as well. The AF results from the model and the local data are compared one to one for each of the input motions. The relative difference in AF is shown in Figure 7 for Amsweer. Each dot represents one coordinate on the 2D line and one motion. The average and the standard deviation are represented by the red lines. The average difference over all periods is 8 % for Amsweer and 18 % for both Biessum and Helwerd. The range of periods between 0.1 and 1.0 s is relevant for the risk assessment. The average difference in AF for the risk relevant periods is 7 %, 17 % and 28 % for Amsweer, Biessum and Helwerd. These numbers generally surpass the commonly acceptable uncertainties indicating the effect of the wierden is significant. AF from the GMM model is lower on average than AF from local data. For all three wierden in the GMM development area, the model without the impact of the wierden therefore underestimates the AF.

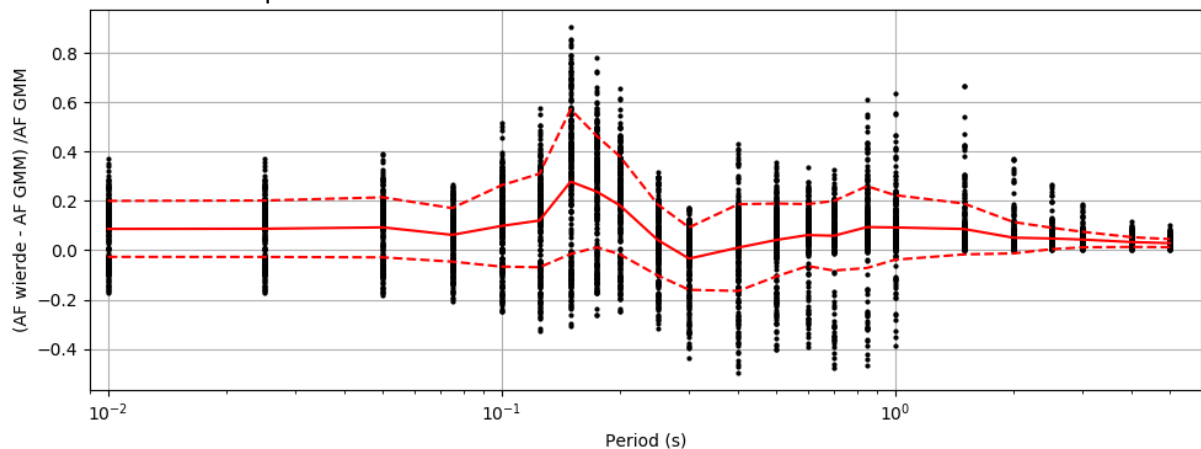


Figure 7 Comparison of AF results per soil column and motion for GMM wierden Amsweer (dots). The solid red line represents the average AF for each period, the dashed red lines indicate plus or minus one standard deviation.

The wierden where MASW measurements were performed both on and off wierden was Groot Maarslag. The 16 m columns were used to compare the site response for these two situations. Figure 7 shows that the AF on the wierden are significantly different from the pasture some distance away from the wierden.

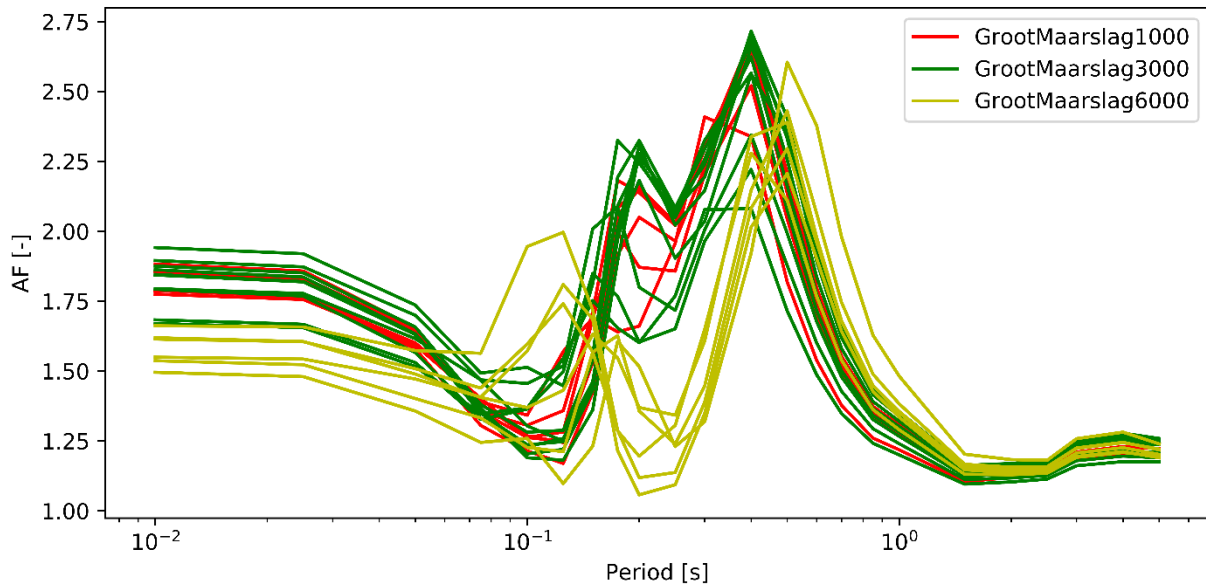


Figure 8 AF results for Groot Maarslag for one representative motion showing the difference in behaviour on wierden (line 1000 and 3000) and off wierden (line 6000).

Next it was checked whether the three wierden in the GMM area are representative of all investigated wierden. An effective penalty function can only be derived when considering the full soil column as is done for the GMM. For the comparison between the individual wierden, all columns have been cut-off at a common reference depth of 16 m, which is the minimum depth range of the 2D V_s profiles. The average AF curves for the 16 m columns are shown in figure 8. All wierden, except for Grote Houw, show similar AF behaviour among periods. Grote Houw shows substantially lower AF compared to the other wierden. This is probably related to the fact that this wierden is much sandier than the other wierden and therefore less prone to amplification. The GMM wierden seem to fall on the high side of the average curve. This means that using the average AF for these three wierden for the full soil column including the antropogenic wierden is a conservative choice.

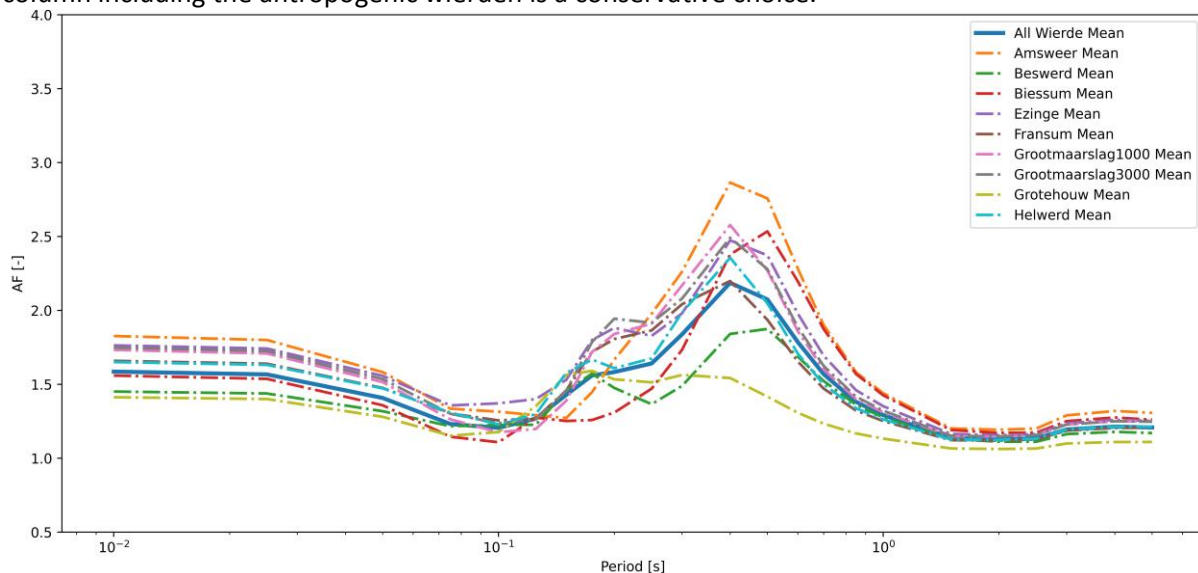


Figure 9 Mean AF result for the 16 m soil columns of all wierden.

Further work

Define the period- or frequency dependent AF penalty function for buildings located on a wierden. This will be completed before 15th November 2020.

Ground Motion Prediction

Seismic data validation

There are a total of 811 records from 29 earthquakes in the magnitude range 2.5 to 3.6. This includes records from two recent events: the Zijldijk earthquake on 2nd May 2020 ($M_L = 2.5$) and the Loppersum earthquake on 14th July this year ($M_L = 2.7$).

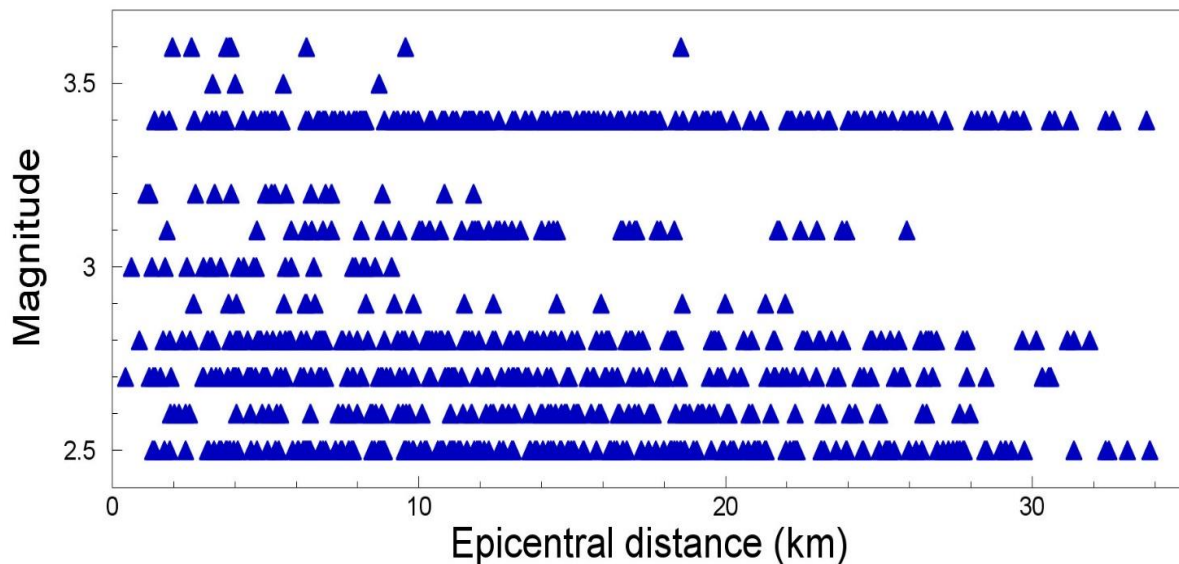


Figure 10 Full set of available records.

A data validation review was carried with extensive interactions with the GMM assurance review panel to establish criteria for inclusion of seismic records and the processing procedures leading to the final database to be used in the development of GMM V7. These records were carefully screened and records not meeting the stringent quality criteria were removed.

The main changes with respect to GMM V6 made in the data used for development GMM V7 are:

- Only recordings from surface instruments were used in the development of the ground motion prediction methods. The borehole instrument recordings are no longer directly used. As a result, the V7 GMM is based on a homogenous dataset and consistent soil profiles for deconvolution and forward modelling.
- Records from malfunctioning instruments were removed: Three G-stations (G050, G530, G680) have malfunctioned, so records from these accelerographs were rejected from the database. Additionally, records obtained from the BLOP station from end 2017 to 2019 were removed since this instrument malfunctioned during that period.
- Records from non-anchored instruments were retained. Records from the BSTD and STDM station, which was found to have not been anchored, were retained because records did not suggest any effect.
- Records from B-stations were retained. For the first 18 (out of 28) earthquakes in the database, the recordings come exclusively from the B-network; the strongest and closest recordings in the database come predominantly from these stations.
- Records from stations placed below ground level were corrected. For these B-stations (BUHZ, BWIN and BZN1), the correction procedures proposed by NIST (2012) were applied to compensate for the embedment effect and recover the 'true' high-frequency motions.

- Recordings from stations without measured Vs profiles were removed. In July 2020, a further third SCPT campaign was carried out to minimise the number of records that needed to be removed, due to lack of a measured soil Vs profile at the station site (Ref 25 and 28).
- Records from stations located outside the study area were removed. Outside this area no shallow geological model is available.
- In processing further recordings were removed. Records were eliminated, if FAS found to have:
 - Lower useable frequency > 2 Hz.
 - Upper useable frequency < 10 Hz.
 - SNR < 3 across frequency range.

For the first 18 (out of 28) earthquakes in the database, the recordings come exclusively from the B-network; the strongest and closest recordings in the database come predominantly from these stations (Fig. 11). A comprehensive study into potential soil-structure-interaction (SSI) for the buildings housing the B-stations was conducted (Ref. 25 and 26). This showed these buildings (apart from those where the stations had been placed in basements) could not have impacted the B-stations recordings. It was hypothesised that the most likely cause for the systematic suppression of short frequency ordinates is a result of enhancement / consolidation of the soil prior to construction or due to local vibrations in combination with the weight of the building increasing Vs locally underneath the building. However, the frequency domain where this effect would be felt is such that impact on typical buildings in Groningen is minimal.

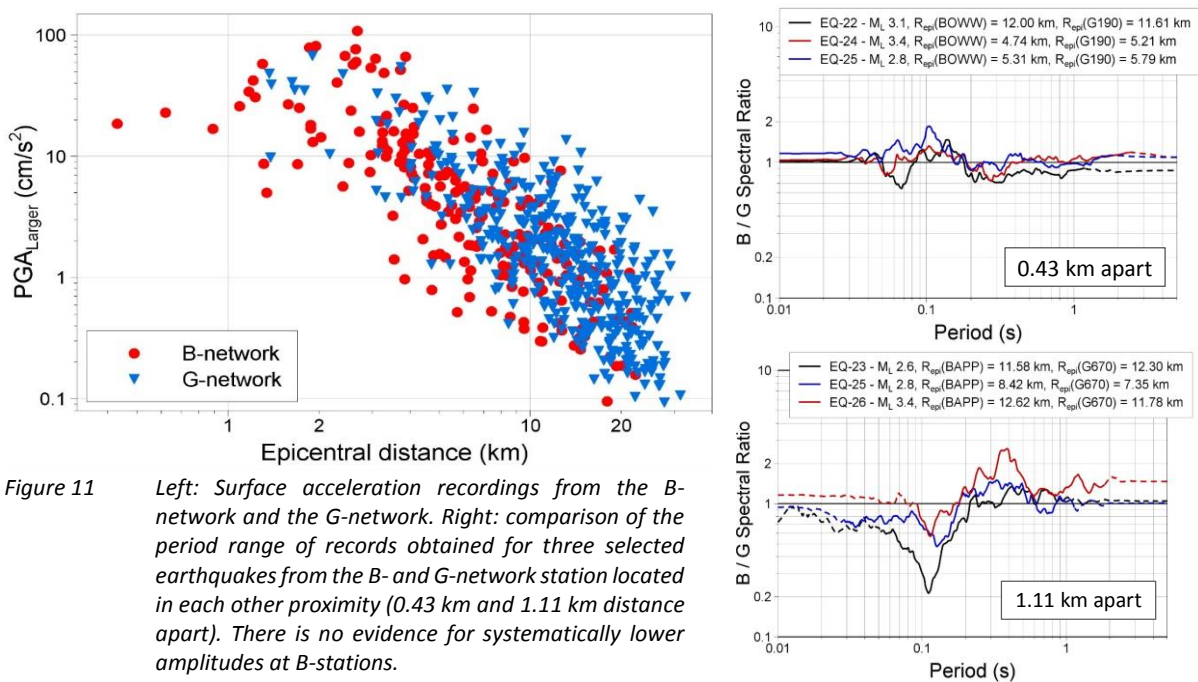


Figure 11 Left: Surface acceleration recordings from the B-network and the G-network. Right: comparison of the period range of records obtained for three selected earthquakes from the B- and G-network station located in each other proximity (0.43 km and 1.11 km distance apart). There is no evidence for systematically lower amplitudes at B-stations.

Measured Vs profiles at B-stations showed that Vs profiles derived from the GeoTop model are surprisingly good, but systematic differences were identified between AFs at B-stations (with measured Vs profiles) and G-stations (with GeoTop-based) AFs.

SCPT measurements performed by Fugro for KEM provided Vs profiles at several G-stations. NAM engaged Fugro to extend the campaign to a much larger number of the G-stations in June 2019 (Ref. 27 to 30). The assurance team, after much internal debate, decided records from G-stations without measured Vs profile should be excluded. NAM re-mobilized Fugro to resume the SCPT campaign, targeting the remaining G-stations producing the most and/or the strongest recordings, which reduced (in an expanded database) the number of excluded recordings.

Study and Data Acquisition Plan 2020 – Addendum
Close-out Report

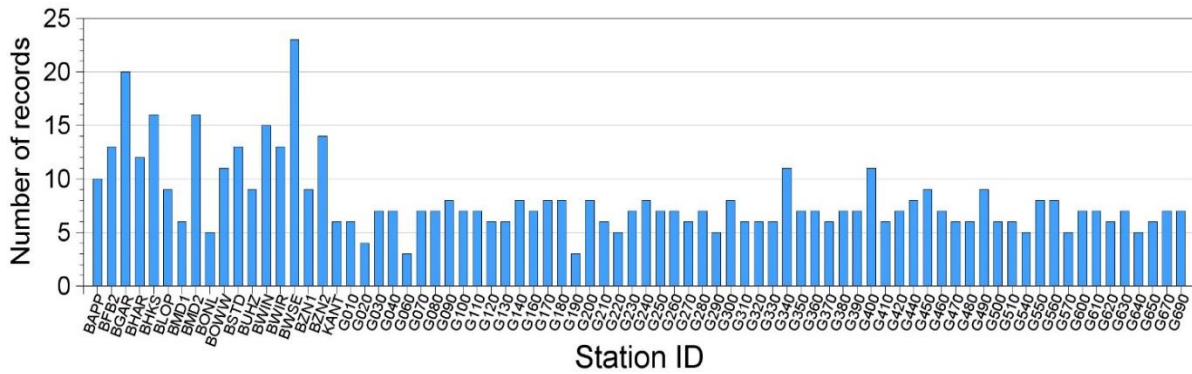


Figure 12 The number of records obtained from each B- and G-network station.

Figure 12 shows the number of seismic records obtained by the individual B- and G-network stations. The G-stations have on average contributed some 7 seismic records, while one of the B-stations has contributed more than 20 seismic records. An overview of the relative offset at three periods (0.01 s, 0.1 s and 0.2 s) shows there is no evidence for systematically lower amplitudes at B-stations, while there is some evidence for suppression of high-frequency motions at B-stations installed in basements (e.g. BUHZ) (Fig 13).

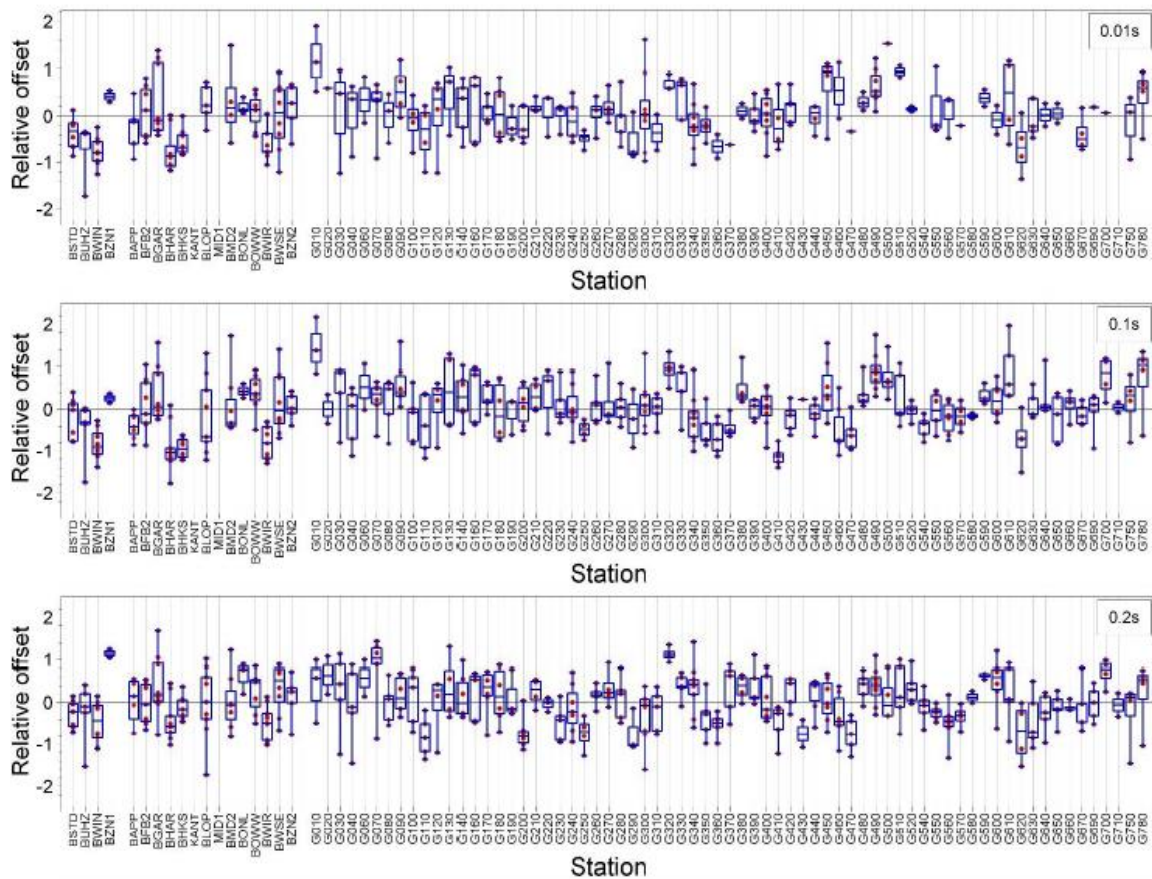


Figure 13 Relative offset at three periods (0.01 s, 0.1 s and 0.2 s) for seismic records obtained from B-network stations and G-network station.

The final database contained 625 seismic recording of 29 earthquakes. Table 1 gives an overview of the number of earthquakes and seismic records available for the development of the different versions of the GMM model.

GMM	Data sources	Database size
V2	(B)	12 events; 106 records
V3	(B – G4)	22 events; 178 records
V4	(B – G4)	22 events; 178 records
V5	(B – G4)	23 events; 258 records
V6	(B – G0)	25 events; 414 records
V7	(B – G0)	29 events; 625 records

Table 1 Number of records obtained from the number of earthquakes for each of the versions of the ground motion prediction methodology. As more seismic records became available more stringent quality screening could be implemented.

Due to the larger database of seismic records available, it was in the development of ground motion prediction method version 7 possible to apply more stringent quality selection criteria in the processing and selection of records. A lower period criteria T_{min} was introduced, while a more stringent T_{max} criteria of 0.7 was used (previously 0.9). As a result of the record processing, the number of available records changes with the period. Figure 14 shows the number of seismic records available at each period. Over the for risk important range, from 0.1 s to 0.5 s, the number of records exceeds 600.

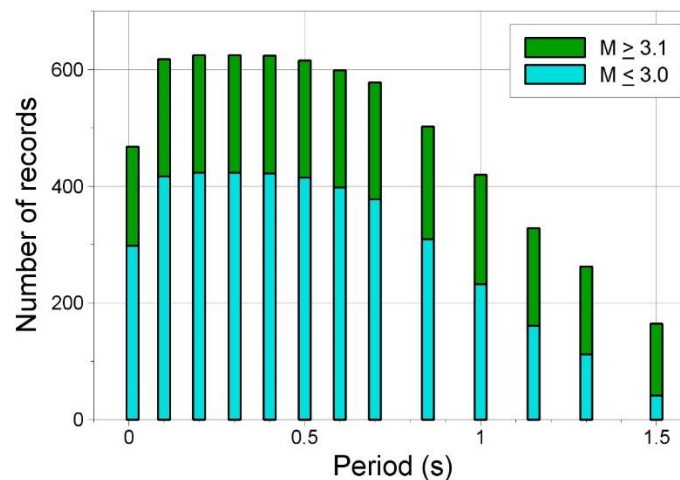


Figure 14 Number of seismic records available in the database for each period.

Shallow formation Properties

Shear wave velocity

The shear wave velocity model that will be used in the development of GMM V7 is predominantly unchanged from that used for GMM V6 (Ref. 15 to 16). Additional data is available as additional SCPT data was obtained. Soil properties are unchanged with the exception of the damping parameters (see next section).

Study and Data Acquisition Plan 2020 – Addendum
Close-out Report

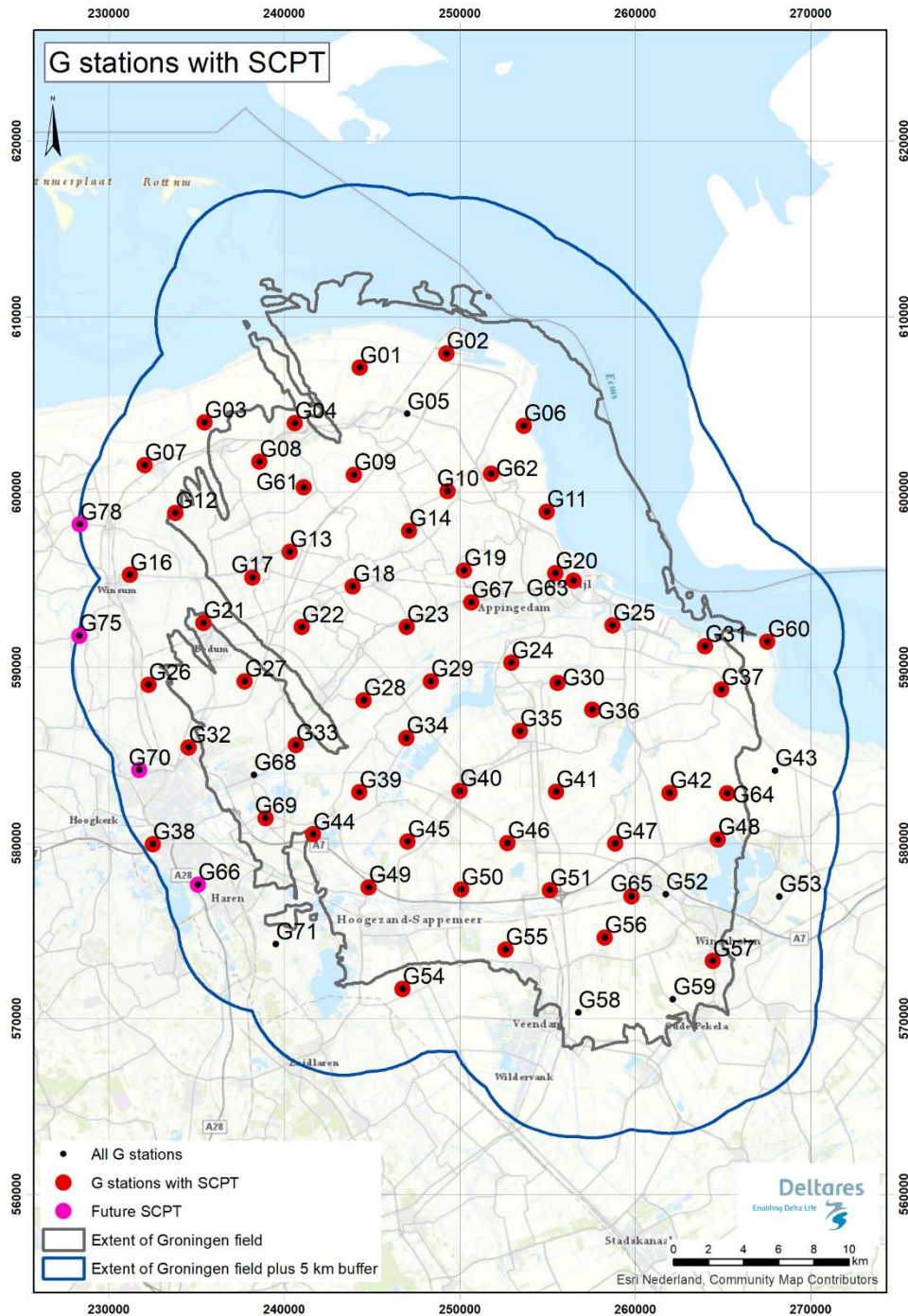


Figure 15 Map of the location of the G-stations with the availability of a SCPT indicated.

In total there have been three campaigns to obtain the SCPT data at the G-station locations:

- An initial set of SCPT were obtained at 14 stations for the KEM-04 project,
- An additional set of SCPT were obtained at 31 stations by NAM in 2019 and
- A final set of SCPT were obtained at 8 stations (in time to be used in the development of GMM V7) by NAM in 2020.

This resulted in a total of 53 SCPTs with varying length, starting at 0.5, 1.0 or 1.5 m below the surface. Not all SCPT cover the full 30 m. This left 15 G stations without an SCPT.

Damping

For the characterisation of the shallow subsurface, especially the small strain damping (Q) is important. The models for damping were progressively developed. Initially for GMM version 2, the damping derived from laboratory experiments by Darendeli (Ref. 31) were used to estimate the damping coefficients for the sand and clay soil types, while a damping coefficient for peat were derived from a study of available literature. These were refined in the development of subsequent versions of GMM. For sand the model by Menq (2003) was used from GMM V3 onwards. Damping estimates obtained in two borehole arrays (De Crook & Wassing 1996, 2001) and other experimental studies indicated that laboratory estimates of D_{min} underestimate the damping needed to match observations in downhole arrays (e.g., Tao and Rathje 2019; Yee et al. 2013; Stewart et al. 2014). In general, damping estimates obtained from borehole experiments implied higher damping than the laboratory-based models indicate. The damping estimates derived from laboratory experiments were therefore multiplied by 2.11 in versions 3, 4 and 5 of the GMM.

For GMM V6, measurements of damping were conducted at the G-stations using seismic interferometry using the methods developed by Snieder and Safak (2006). Seismic interferometry models a source at the borehole sensor and obtains the transfer function by deconvolution using local seismicity [2-20 Hz range]. Results of this interferometry gave higher values of damping than in previous models.

Comparison of the GMM V5, which was developed based on B-stations surface accelerometers and the G4-station deepest geophones, with GMM V6, developed based on surface accelerometers only, prompted further study into the characterisation of the damping in the shallow soil formations. In support of the development of V7 GMM, studies were performed by KNMI to estimate damping (Q). At several stations, damping was estimated using two methods:

- Seismic interferometry was used (as in GMM V6), with improvements and
- ‘Up-and-Down’ method was additionally used (Fukushima et al. 2016; Haendel et al. 2019)

In the ‘Up-and-Down’ damping estimation scheme, a single sensor is used to estimate Q using the up-going and down-going wave. For a synthetic, perfectly elastic deconvolution (no damping), the up-going and down-going amplitudes would be identical (Fig. 16).

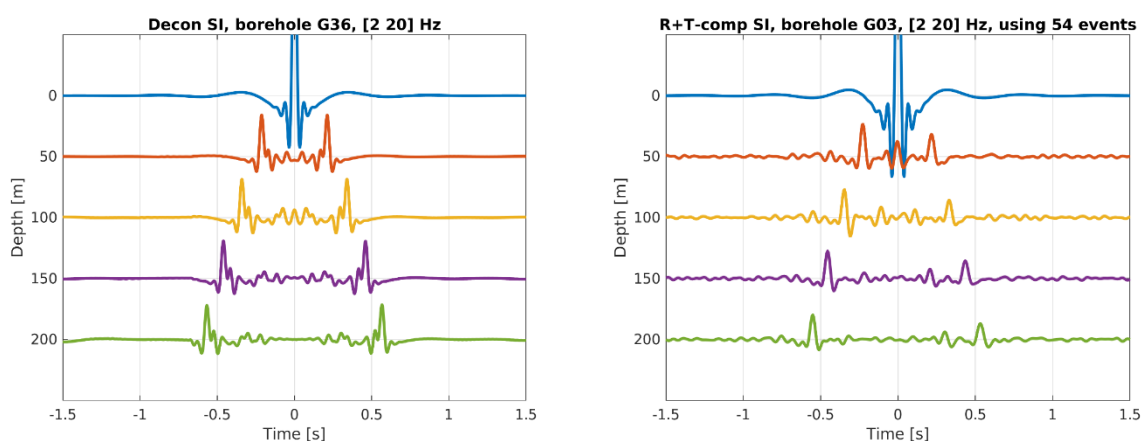


Figure 16 Synthetic perfectly elastic deconvolution result. For a synthetic, perfectly elastic deconvolution (no damping), the up-going and down-going amplitudes would be identical (see plot on left). When damping is added, the amplitude of down-going wave is reduced (see plot on right).

Results obtained with the ‘Up-and-Down’ method were more physical than with those of the interferometry approach.

- No negative damping Q-values were generated and
- In generally, the damping Q-values increase with depth.

Results we found to be more reliable because any amplitude measurement error in an instrument gets cancelled out in the ‘Up-and-Down’ method. As a result the damping Q estimates obtained with the ‘Up-and-Down’ approach were used in the development of GMM V7.

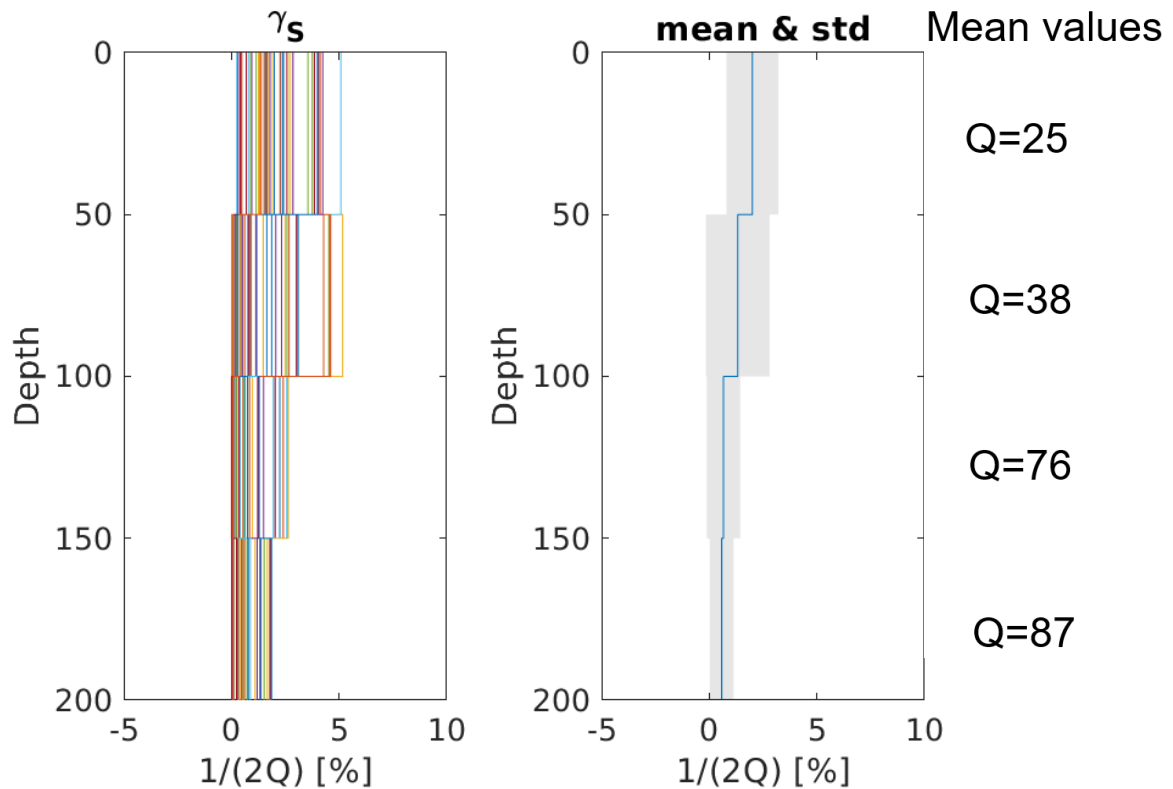


Figure 17 Vertical damping profiles for the G-stations.

Further Work

The development of GMM V7 is currently in progress. This is done with active steering from the Assurance Committee. The preparation of the database and estimation of key parameters has been completed.

Table 2 shows the planning of the activities for the development of ground motion prediction methodology version 7 (GMM V7). These are divided over four main work packages with dedicated deliverables. The preparation of the main building block for the development have been completed. These are the preparation of the database of seismic records and the improvements of the characterisation of the shallow geological layers, in particular damping coefficients. This has been described in this report.

The second work package (central model calibration) is currently being finalised. Work on the third works package (model generation with epistemic uncertainty) is ready to commence. Definition of the logic tree is currently in progress. This work package will be finalised before the end of 2020. Early November 2020, a workshop will be held with TNO to facilitate incorporation of the ground motion prediction methodology into the hazard and risk assessment.

Documentation of the development of version 7 of the GMM will be finalised in January 2021. Where previous reports (since the report on GMM V4) primarily focussed on the improvements of the GMM,

Study and Data Acquisition Plan 2020 – Addendum
Close-out Report

the report on V7 will be a full documentation of the ground motion prediction methodology without reference to previous reports.

Basic building blocks	<ol style="list-style-type: none"> 1. Identify deliverables. SA(T) at 13 periods from 0.01 to 1.5 seconds 2. Record processing. Criteria to define T_{min} and T_{max}; minimum SNR criterion 3. Record selection. Which stations to include (basements, no V_s, etc.) 4. Final V_s model. Updated model based on new measurements and refinements 5. Database compilation. Flat-file of SA(T) and metadata 6. Damping model. Final model for low-strain damping in soil profiles 	Completed
Central model calibration	<ol style="list-style-type: none"> 7. TFs for FAS at NS_B. Transfer functions from surface to NS_B at recording stations 8. FAS at NS_B. Fourier amplitude spectra at NS_B 9. Inversion of NS_B FAS. Inversion of FAS for source, path and site parameters 10. Simulated FAS at NS_B. Simulated FAS at NS_B for all M-R as input to AF calculations 11. AFs for recording stations. Scenario-dependent AFs for all recording stations in the V7 database 12. Response spectra at NS_B. Apply AFs from #11 to provide response spectra at NS_B to Ben 13. Parameterisation of EXSIM simulations. Source, path and site parameters for simulations. 14. Calibration of central model simulations. Stress and kappa parameters to match NS_B RS 15. Forward simulations of NS_B RS. Simulate RS at the NS_B horizon for all M-R combinations 16. Refined scenario-dependence of AFs. Revise M-R dependence of AFs using simulated motions 17. Revised RS at NS_B. Repetition of steps #12 and #14 using updated AFs from #16. 	Method Agreed / In Progress: Oct. – Nov.
Model generation with epistemic uncertainty	<ol style="list-style-type: none"> 18. NS_B logic-tree structure. Definition of logic-tree structure for forward simulations 19. Logic-tree for site response model. Define branches and models for site response calculations 20. Simulation of NS_B FAS. Generate NS_B FAS for all M and R, using all branches of logic-tree 21. Strata calculations. Calculate AFs for all voxels and all logic-tree branches, using inputs from #20 22. AFs and zonation. Check zonation and derive nonlinear AFs for all zones and all spectral periods 23. Simulated RS as NS_B. Simulated RS for all M-R combinations and all logic-tree branches 24. NS_B GMPE. Regressions on simulated RS at NS_B with appropriate functional form 25. Sigma model. Model for variability in NS_B and surface motions, informed by #22 and #24 26. Final logic-tree branch weights. Weights on branches for medians & sigmas at NS_B and surface 	Assurance Team / Planned for Nov.
Documentation	<ol style="list-style-type: none"> 27. Summary of V7 GMM. Brief summary of model for HRA team 28. V7 GMM report. Comprehensive documentation of final V7 GMM 	Planned for Dec. – Jan.

Table 2 Activities and work packages for the development of ground motion prediction methodology version 7.

Extension of the database of seismic records to additionally include the earthquakes in the magnitude range $M=1.8$ to $M=2.5$ is in progress. The extended database will be the basis for the update of empirical GMPE.

Seismological Model

Areal and temporal distribution of earthquakes

The recent advances in the determination of the hypocentre location of earthquakes (Ref. 32 and 33) also allowed determination of the source mechanisms for a catalogue of some 200 earthquakes. The following datasets have been used in the construction and calibration of the seismological model:

- (1) the strain data as derived from subsidence,
- (2) the reservoir pressure data from the dynamic model of the reservoir,
- (3) the topographic gradient from the static model of the reservoir and
- (4) the earthquake catalogue with event time, location and magnitude.

The catalogue of earthquakes with a seismic moment tensor observation allows for further extension and refinement of the seismological model. Including the earthquake source mechanism (and therefore orientation) is potentially important as this might indicate how any stress anisotropy might favour one fault orientations in the field over others and therefore impact the forecast of the earthquake density.

The equations for poro-elastic thin-sheet deformations induced by pore pressure changes for seismological model (V5 and V6) (Ref. 34 and 35) were limited to optimally oriented faults with zero pre-stress anisotropy. In the further development of this model these thin-sheet equations will be generalised for any fault orientation with anisotropic pre-stress.

Further Work

The stress-dependent activity rate and magnitude models are coupled to a scalar poro-elastic thin-sheet stress model. This choice of a scalar stress model is suitable to model the stress-dependence of event origin times, locations and magnitudes with smoothing length-scales in the range 3—5 km which are considerably larger than the typical spacing between individual pre-existing faults. With the emergence of an increasing large catalogue of seismic moment tensor observations that may indicate preferential reactivation of fault segments that are preferentially oriented for failure under the combination of the initial pre-stress tensor and the local induced incremental stress tensor. In this manner the distribution of observed focal mechanisms may reflect the spatial-temporal evolution of the total stress tensor. In turn the observed focal mechanisms may be used to constrain the pre-stress anisotropy and a tensorial poro-elastic thin-sheet incremental stress model. This type of model may better constrain the strike orientations of induced seismicity forecasts and may also modify the spatial distribution of modelled epicentres by restricting activity to a limited distribution of optimally oriented pre-existing fault strikes.

Action: Extend the existing analytic, scalar, poro-elastic, thin-sheet model to include tensorial pre-stress and tensorial incremental stresses due to reservoir pore pressure changes and reservoir compaction strains. Seek to constrain this model using the observed catalogue of seismic moment tensors and to extend seismological forecast capabilities to include seismic moment tensors. This study will be completed in 2021 and therefore not be included into the hazard and risk model for HRA 2012.

Stress-Dependent Magnitudes

Version six of the seismological model addresses the distribution of earthquakes over the magnitude range (Ref. 45) and was shared with TNO, KNMI, SodM and the international assurance panel in October 2019. A report describing the model update and the assurance reviews were shared on NAM's public webpage in November 2019 and January 2020 respectively. Based on discussions with the development team of this seismological model, own internal assurance and the international

assurance reviews (Ref. 46), SodM advised to use this model for the hazard and risk assessment due March 2020. In response to this advice the Minister instructed NAM to use this version of the seismological model in the expectation letter of February 2020. In May 2020, TNO issued a critical review of the model (Ref. 47) in its advice to the Minister. This TNO review together with a response by NAM were shared with the international assurance panel for their opinion.

The members of the assurance panel in their review all supported the Seismological Model (V6) and reconfirmed it to be the most appropriate choice for inclusion in the HRA at this point in time. They also identified a couple of areas for further study of induced seismicity in Groningen. In this section, two suggestions for follow-up studies are discussed. Both the recommendations from the assurance panel will be carried out as part of the Study and Data Acquisition Plan.

Further Work based on discussion with the Assurance Panel

Both the activity rate model and the magnitude models are stress dependent. The space-time evolution of stress within the reservoir due to Groningen gas production is modelled using a fast, analytic, poro-elastic, thin-sheet model that allows very large numbers of alternative model instances to be investigated. These alternative reservoir stress models are parameterized by three variables. The first parameter is the length-scale of spatial smoothing applied to these stress fields. The second is a fault filtering parameter that excludes some faults from the seismological model due to aseismic slip according to their juxtaposition of the reservoir formation against the overlying ductile Zechstein salt formation. The third parameter is a poro-elastic modulus that governs the relative contributions of reservoir pore pressure changes and reservoir compaction strains to the vertically averaged, incremental, maximum Coulomb stress states within the reservoir. The joint probability distribution of these poro-elastic thin-sheet stress model parameters was first obtained in combination with the stress-based extreme threshold activity rate model using Bayesian inference given the observed event locations and origin times. Subsequently, a separate joint probability distribution of these poro-elastic thin-sheet stress model parameters was obtained in combination with the stress-based magnitude models using Bayesian inference given the observed event magnitudes. These two independent inferences of the poro-elastic thin-sheet stress model resulted in different joint probability distributions for the model parameter values. The resulting stress fields from these two different stress models are similar in their relative spatial distributions and temporal evolutions. The remaining differences may simply reflect differences in the statistical resolving power of the activity rate observations relative to the magnitude observations. However, it does raise the possibility that a single stress model obtained by joint inference with both the stress-dependent activity rate model and the stress-dependent magnitude model might improve the constraints on the stress model parameter values in a manner that also improves the out-of-sample forecast performance of both the stress-dependent activity rate model and the stress-dependent magnitude model.

Action: Evaluate the performance of joint inference of a single elastic thin-sheet stress model shared with both the stress-dependent seismological activity rate model and the stress-dependent magnitude model.

The Kolmogorov-Smirnov test splits the observed earthquake magnitudes into two parts with significantly different frequency-magnitude distributions. This division was made based on the local modelled reservoir stress state. These two sets of events appear to be more separated in their spatial distribution than their temporal distribution. However, there is still a clearly observable spatial overlap where some earlier lower stress events occurred in places surrounded by later higher stress events. Although it seems unlikely that some form of stress-invariant structural heterogeneity would happen to be co-located within the region of largest modelled stress increases, this possibility was not yet investigated.

Study and Data Acquisition Plan 2020 – Addendum
Close-out Report

Action: Investigate the possible role of resolvable structural heterogeneity as a stress-invariant control on spatial variations in beta- and zeta-values. Explore methods for mapping any time-invariant spatial variations in beta- or zeta-values, or joint variations in both beta- and zeta-values. Then use these time-invariant beta-value maps and zeta-value maps to develop alternative stress-invariant magnitude models that included beta- and zeta-value spatial variations that might be controlled by pre-existing structural heterogeneities such as fault roughness or elastic modulus variations.

References

1. Study and Data Acquisition Plan Induced Seismicity Groningen 20219, Jan van Elk, Dirk Doornhof and Jeroen Uilenreef, NAM, January 2019.
2. Letter: Betreft beoordeling “Study and Data Acquisition Plan” incl. addendum, 17 December 2019, SodM.
3. Letter: Betreft beoordeling “Study and Data Acquisition Plan” incl. addendum, 12 February 2020, NAM.
4. Study and Data Acquisition Plan Induced Seismicity Groningen 2020 - Executive Summary, Jan van Elk, Dirk Doornhof and Jeroen Uilenreef, NAM, September 2020.
5. Study and Data Acquisition Plan Induced Seismicity Groningen 2020 - Part 1: Introduction and Credibility Process, Jan van Elk, Dirk Doornhof and Jeroen Uilenreef, NAM, September 2020.
6. Study and Data Acquisition Plan Induced Seismicity Groningen 2020 - Part 2: Subsurface Discovery Process, Jan van Elk and Dirk Doornhof, NAM, September 2020.
7. Study and Data Acquisition Plan Induced Seismicity Groningen 2020 - Part 3: Impact at Surface Discovery Process, Jan van Elk and Jeroen Uilenreef, NAM, September 2020.
8. Letter: Betreft beoordeling “Study and Data Acquisition Plan” update 1 July 2020, SodM, 15 September 2020.
9. A geological history of Groningen’s subsurface, Erik Meijles, Rijksuniversiteit Groningen, NAM, June 2015.
10. De ondergrond van Groningen: een geologische geschiedenis, Erik Meijles, Rijksuniversiteit Groningen, NAM, June 2015.
11. Terp composition in respect to earthquake risk in Groningen, Dr. ir. E.W. Meijles, Dr. G. Aalbersberg, and Prof. dr. H.A. Groenendijk, RUG, Mar 2016.
12. Report Erik Meijles
13. Report on soil-structure interaction (SSI) impedance functions for SDOF systems, Roberto Nascimbene, Rui Pinho and Helen Crowley, mosayk, Jan 2015.
14. Calibration and verification of a nonlinear macro-element for SSI analysis in the Groningen region, Francesco Cavalieri, António A. Correia, Mosayk, Apr 2019.
15. V6 Ground-Motion Model (GMM) for Induced Seismicity in the Groningen Field - With Assurance Letter, Julian J Bommer, Benjamin Edwards, Pauline P Kruiver, Adrian Rodriguez-Marek, Peter J Stafford, Bernard Dost, Michail Ntinalexis, Elmer Ruigrok and Jesper Spetzler, Dec 2019.
16. Coefficient files for V6 Ground-Motion Model (GMM) for Induced Seismicity in the Groningen Field, Julian J Bommer, Benjamin Edwards, Pauline P Kruiver, Adrian Rodriguez-Marek, Peter J Stafford, Bernard Dost, Michail Ntinalexis, Elmer Ruigrok and Jesper Spetzler, Dec 2019.
17. Geological schematisation of the shallow subsurface of Groningen. For site response to earthquakes for the Groningen gas field. part 1, Pauline Kruiver, Ger de Lange, Ane Wiersma, Piet Meijers, Mandy Korff, Jan Peeters, Jan Stafleu, Ronald Harting, Roula Dambrink, Freek Busschers and Jan Gunnink, Deltares and NAM, June 2015.
18. Geological schematisation of the shallow subsurface of Groningen. For site response to earthquakes for the Groningen gas field. part 2, Pauline Kruiver, Ger de Lange, Ane Wiersma, Piet Meijers, Mandy Korff, Jan Peeters, Jan Stafleu, Ronald Harting, Roula Dambrink, Freek Busschers and Jan Gunnink, Deltares and NAM, June 2015.
19. Geological schematisation of the shallow subsurface of Groningen. For site response to earthquakes for the Groningen gas field. part 3, Pauline Kruiver, Ger de Lange, Ane Wiersma, Piet Meijers, Mandy Korff, Jan Peeters, Jan Stafleu, Ronald Harting, Roula Dambrink, Freek Busschers and Jan Gunnink, Deltares and NAM, June 2015.
20. Modifications of the Geological model for Site response at the Groningen Field, P. Kruiver, Deltares, June 2016.
21. Assessment of dynamic properties for peat - Factual Report, dr.ir. C. Zwanenburg and M. Konstantinou, Deltares, Oct 2017.
22. Dynamic behaviour of Groningen peat - Analysis and parameter assessment, M. Konstantinou, dr.ir. C. Zwanenburg and dr.ir. P. Meijers, Deltares, Oct 2017.
23. Background document NAM database of subsurface information - Version date of database - 29 March 2018, Pauline Kruiver, Fred Kloosterman, Ger de Lange, Pieter Doornenbal, Deltares, Mar 2018.
24. CPT in Thinly Layered Soils - Validation Tests and Analysis for Multi Thin Layer Correction, D.A. de Lange, Deltares, Aug 2018.

Study and Data Acquisition Plan 2020 – Addendum Close-out Report

25. Soil-structure-interaction analysis in support of Groningen - B-stations verification efforts, Francesco Cavalieri, António A. Correia, Mosayk, May 2020.
26. Soil-structure-interaction analysis in support of Groningen - B-stations verification efforts – including basement correction and comments from Assurance Panel, Francesco Cavalieri, António A. Correia, Mosayk, October 2020.
27. Campaign to acquire SCPT at the location of the G-stations of the Seismic Monitoring Network (operated by KNMI), FUGRO, FUGRO, Nov 2019.
28. Digital data campaign to acquire SCPT at the location of the G-stations of the Seismic Monitoring Network (operated by KNMI), FUGRO, FUGRO, Nov 2019.
29. Digital data second campaign to acquire SCPT at the location of the G-stations of the Seismic Monitoring Network (operated by KNMI), FUGRO, FUGRO, Aug 2020.
30. Second Campaign to acquire SCPT at the location of the G-stations of the Seismic Monitoring Network (operated by KNMI), FUGRO, FUGRO, Aug 2020. An activity rate model of induced seismicity within the Groningen Field, Stephen Bourne and Steve Oates, Shell, Sept 2014.
31. Darendeli
32. Empirical Green's Function analysis of some induced earthquake pairs from the Groningen gas field, Steve Oates, Jelena Tomic, Brian Zurek, Tom Piesold and Ewoud van Dedem, Shell/Exxonmobil, Aug 2020.
33. Determination of Hypocentre location using Full Waveform Inversion – including catalogue of earthquakes., Chris Willacy and Jan Willem Blokland, Shell, Sept 2020.
34. An activity rate model of induced seismicity within the Groningen Field (Part 1), Stephen Bourne and Steve Oates, Shell, July 2015.
35. An activity rate model of induced seismicity within the Groningen Field (Part 2), Stephen Bourne and Steve Oates, Shell, July 2015.
36. Computing the Distribution of Pareto Sums using Laplace Transformation and Stehfest Inversion, Chris Harris, Shell and NAM, Aug 2015.
37. Induced seismicity in the Groningen field - A statistical assessment of tremors along faults in a compacting reservoir, Rick Wentinck, Shell and NAM, Nov 2015.
38. Maximum Likelihood Estimates of b-Value for Induced Seismicity in the Groningen Gas Field, Chris Harris and Stephen Bourne, NAM/Shell Global Solutions, Nov 2015.
39. Local and Moment Magnitudes in the Groningen Field, Bernard Dost, Julian Bommer and Ben Edwards, July 2016.
40. Reader for the Spatial and Temporal development of induced seismicity in the Groningen field, S.J. Bourne, S.J. Oates, NAM, Nov. 2017.
41. Evaluation of a Machine Learning methodology to forecast induced seismicity event rates within the Groningen Field, J. Limbeck, F. Lanz, E. Barbaro, C. Harris, K. Bisdorn, T. Park, W. Oosterbosch, H. Jamali-Rad and K. Nevenzeel, IBM/Shell, Aug 2018.
42. A New Maximum-Likelihood Method for Determining The Correlation Dimension of Clusters of Seismic Events – Application to Groningen, Chris Harris and Stephen Bourne, NAM, Nov 2018.
43. Characterization of Induced Seismicity using Fiber Bundle Models, Chris Harris and Stephen Bourne, NAM, Nov 2018.
44. Gaussian Process Optimisation of the Elastic Thin-Sheet Seismological Model for Depletion Induced Seismicity in the Groningen Gas Field, G. Joosten, J. Limbeck, G. Kaleta, S. Bourne, K. Nevenzeel, Shell Research and IBM Services, Feb 2019.
45. Evolution of induced earthquake magnitude distributions with increasing stress in the Groningen gas field, S.J. Bourne, S.J. Oates, NAM, Dec 2019.
46. Assurance of the report: Evolution of induced earthquake magnitude distributions with increasing stress in the Groningen gas field by Stephen Bourne and Steve Oates, S.J. Bourne, S.J. Oates, NAM, Jan 2020.
47. Advice by TNO on the seismological model for the Hazard and Risk Assessment for induced seismicity in Groningen, TNO, May 2020.

Study and Data Acquisition Plan 2020 – Addendum
Close-out Report